Chinese Chemical Letters 37 (2026) 111617

Contents lists available at ScienceDirect

Chinese Chemical Letters

journal homepage: www.elsevier.com/locate/cclet

Facile and regioselective B–H bond functionalization of carboranes *via* cage···I(III) interaction

Ping Zhang[a], Hongyuan Ren[a], Zhaofeng Sun[a], Hou-Ji Cao[e], Deshuang Tu[a,*], Chang-Sheng Lu[a,*], Jordi Poater[b,c,*], Miquel Solà[d,*], Hong Yan[a,*]

[a] *State Key Laboratory of Coordination Chemistry School of Chemistry and Chemical Engineering Nanjing University, Nanjing 210023, China*
[b] *Departament de Química Inorgànica i Orgànica & IQTCUB, Universitat de Barcelona, Martí i Franquès 1-11, Barcelona 08028, Spain*
[c] *ICREA, Pg. Lluís Companys 23, Barcelona 08010, Spain*
[d] *Institut de Química Computacional i Catàlisi and Departament de Química, Universitat de Girona, C/Maria Aurèlia Capmany 69, Girona 17003, Catalonia, Spain*
[e] *School of Chemistry and Chemical Engineering, Henan Normal University, Xinxiang 453007, China*

ARTICLE INFO

Article history:
Received 6 May 2025
Revised 24 June 2025
Accepted 19 July 2025
Available online 21 July 2025

Keywords:
Carboranes
B–H functionalization
Boron chemistry
Boron cluster-based luminogens
Aggregation induced emission

ABSTRACT

The development of innovative strategies for inert B–H bond functionalization of carboranes and exploration of their potential applications represents a central task in organic chemistry. Here, we demonstrate the facile B–H bond functionalization in carboranes through a cage···I(III) interaction between a *nido*–carborane cluster and a hypervalent iodine(III) unit. Both experimental and theoretical investigations reveal that the cage···I(III) interaction induces a charge transfer from the boron cage to the iodine moiety, which leads to a significant decrease of the negative charge at the B(9)–H site of *nido*–carborane. This facilitates the activation of the B–H bond and subsequent chemical transformations. The unprecedented cage···I(III) interaction offers a similar B–H bond activation mode as metal mediation. Furthermore, the treatment of *nido*–carboranes with the iodide(III) reagent of $PhI(OAc)_2$ affords *nido*–carborane-phenyl iodonium zwitterions as versatile synthons, which enable the modular construction of exopolyhedral B–O, B–N, B–P, and B–S bonds of carborane derivatives. This approach provides an efficient and scalable synthetic platform for metal-free and site-selective B–H bond functionalization of *nido*–carboranes under mild conditions. Notably, the developed 2D-3D fused structures can be used as ligands for the facile construction of novel boron cluster-fused hetero-polycyclic metal complexes in one step. These compounds demonstrate intriguing photophysical properties including aggregation-induced emission, tunable emission wavelength, and oxygen sensing.

© 2026 Published by Elsevier B.V. on behalf of Chinese Chemical Society and Institute of Materia Medica, Chinese Academy of Medical Sciences.

Boron clusters, such as carboranes, possess three-dimensional (3D) aromaticity and hold immense potentials in materials [1–15], catalysis [16–19], drug design [20–31], and organometallic complexes [32–40]. Hence, the functionalization of boron clusters is of vital importance. However, the presence of multiple inert B–H bonds in similar chemical environments poses a considerable challenge for the synthesis of carborane derivatives [41]. Until now the selective and efficient B–H bond functionalization of carboranes has received tremendous research interest [42–82]. Over the past decades, metal-mediated B–H bond activation has become a prevalent strategy for the functionalization of carboranes owing to the robust capability of the metal that enables weakening of a B–H bond through the formation of a B–M bond for further transformations (Fig. 1a) [42–66]. This approach has facilitated the synthesis of carborane-based functional molecules with distinctive physicochemical properties, such as boron cluster-extended heterocycles (Fig. 1b) [64–66]. Despite the effectiveness of this approach, external ligands, additives or harsh reaction conditions are generally required [42–66]. In contrast, metal-free tactics are capable of overcoming these limitations, therefore being highly attractive [67–83].

It is well recognized that favorable non-covalent interactions play a critical role in synthetic chemistry, particularly in controlling regioselectivity or site-selectivity. Given the established significance of halogen bonding in activating inert bonds [84–89], this study explores metal-free B–H bond functionalization through non-covalent interactions with halogen-containing molecular motifs. In doing so, we identified a type of boron cluster-based non-covalent

* Corresponding authors.
E-mail addresses: tudeshuang@nju.edu.cn (D. Tu), luchsh@nju.edu.cn (C.-S. Lu), jordi.poater@ub.edu (J. Poater), miquel.sola@udg.edu (M. Solà), hyan1965@nju.edu.cn (H. Yan).

https://doi.org/10.1016/j.cclet.2025.111617
1001-8417/© 2026 Published by Elsevier B.V. on behalf of Chinese Chemical Society and Institute of Materia Medica, Chinese Academy of Medical Sciences.

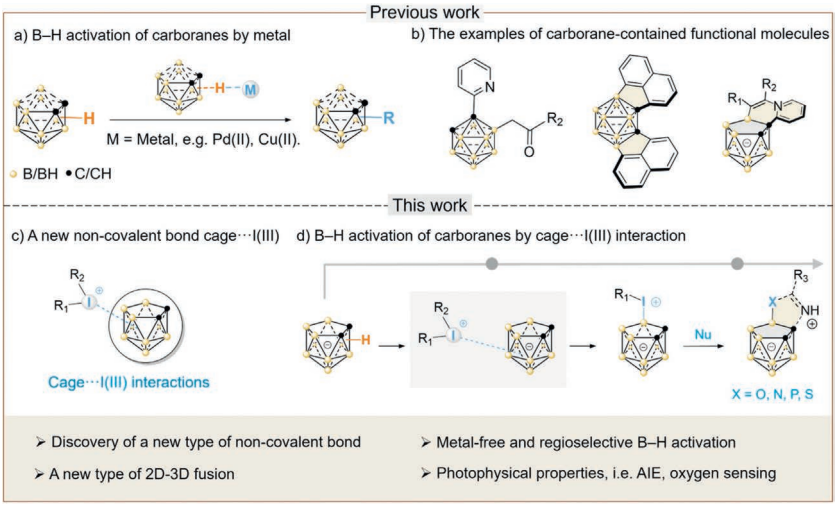


Fig. 1. (a) Classical metal-induced B–H bond activation. (b) The selected carborane-based functional molecules accessed through metal-mediated B–H bond activation. (c) A boron cluster-based non-covalent bond between the 3D aromatic *nido*–carborane and the iodine(III)-containing unit. (d) The B–H functionalization *via* cage···I(III) interaction.

bond, defined as the cage···I(III) interaction, arising from the interaction between a *nido*–boron cluster and a hypervalent iodine unit (Fig. 1c). Single-crystal X-ray diffraction (SCXRD) studies and spectral data indicated the formation of a well-defined electron donor-acceptor complex between the *nido*–carborane and the hypervalent iodine unit.

Further theoretical calculations demonstrated that this bonding involves significant charge transfer, which reduces the negative charge on the B(9)–H of *nido*–carborane, thus facilitating subsequent B–H bond functionalization and transformations. Finally, the metal-free and site-selective B–H functionalization of carboranes has been achieved to lead to the facile formation of B–N, B–P, B–O, and B–S bonds (Fig. 1d). Additionally, a new category of boron cluster-extended skeleton in the form of 2D-3D fused hetero-polycyclic structure has been generated (Fig. 1d). Such an advanced framework enables the facile construction of novel functional molecules that show aggregation-induced emission (AIE) or oxygen sensing.

Carboranes are boron cluster species featuring three-dimensional aromaticity [41,90], which differs from planar aromatic rings. Recently, we have demonstrated that the *nido*–carborane cluster can serve as a novel bonding unit for the construction of non-covalent interactions, such as the cage···π interaction [91]. Given the fact that the research on non-covalent interactions involving boron clusters remains limited [91–93], we are interested in the continuous exploration of new types of boron cluster-based non-covalent interactions. On the other hand, iodine is an important element, which has been extensively involved in functional molecules [94–97]. Notably, the manipulation of the bonding type of iodine would influence the electronic structures of iodine-containing compounds. To investigate the possible cage···I(III) interaction between a boron cluster and an iodine-containing unit, the *nido*–carborane was chosen to interact with an electrophilic iodine compound. Along this line, the hypervalent iodine-supported *nido*–carborane derivatives of **3–1** and **3–2**, as shown in Figs. 2a and b, were synthesized through ion exchange reactions (see Supporting information for synthesis details).

With these compounds in hand, we began to analyze the crystal structures to shed light on the structural characteristics of the cage···I(III) interaction as depicted in Figs. 2a and b. The *nido*–carborane anion is surrounded by several hypervalent iodine cations in both **3–1** and **3–2** due to the electrostatic interactions, as shown in the packing structures (Figs. S18 and S19 in Supporting information) with the carborane cage oriented towards the backside of the V-shaped organoiodine(III) moieties. Moreover, various intermolecular contacts such as C–H···B–H are observed in the crystal structures, collectively endowing a robust non-covalent bonding network for the formation of the cage···I(III) interaction. With careful inspection, the cage···I(III) interaction with a bonding distance of 4.813 Å is identified for **3–1** (measured from the centroid of the boron cage to the iodine atom), alongside B–H···I and B···I contacts with distances of 2.896 and 3.547 Å (Fig. 2a), respectively. A shorter cage···I(III) bonding distance of 4.753 Å is detected for **3–2**, with B–H···I interactions at 2.741 and 2.958 Å, and B···I interactions at 3.401 and 3.966 Å (Fig. 2b), respectively. These indicate that the cage···I(III) interaction can be influenced by the substituents of the aryl hypervalent iodine derivatives.

To further confirm the electronic interaction between the *nido*–carborane and the hypervalent iodine unit, we investigated the UV–vis absorption spectra of **3–2** in both methanol and the crystalline state (Figs. 2c and d). The potassium salt of *nido*–carborane (**1**) and diphenyliodonium trifluoromethanesulfonate (**iodonium-2**) were selected as control compounds. As shown in Fig. 2c, no absorption peak over 250 nm was detected for **1** in methanol. In contrast, the absorption peaks around 260 nm for **iodonium-2** and **3–2** were observed, which correspond to the $\pi \rightarrow \pi*$ transitions of the phenyl substituents. Notably, **3–2** exhibits a new charge transfer absorption band in the 320–400 nm due to the electron donating-accepting interaction between *nido*–carborane and hypervalent iodine groups (Fig. 2c). The charge transfer absorption band is more clear for **3–2** in the crystalline state (Fig. 2d). The spectral results were further validated by the theoretical calculations using the time-dependent density functional theory (TD-DFT) methods (Fig. S24 in Supporting information). Moreover, results from Job's plot indicates a 1:1 stoichiometric association between the iodonium ion and *nido*–carborane anion under the experimental conditions (Fig. S13 in Supporting information). These observations indicate efficient electronic communication between the *nido*–carborane and the hypervalent iodine cation. Due to the unique electronic structures of boron clusters [98–102], further theoretical calculations are conducted to gain a deeper understanding of these intermolecular interactions.

The interactions between the boron cage and the hypervalent iodine moiety for **3–1** and **3–2** have been analyzed by means of the ZORA-BLYP-D3(BJ)/TZ2P dispersion-corrected functional (see Supporting information for computational details). In particular, the

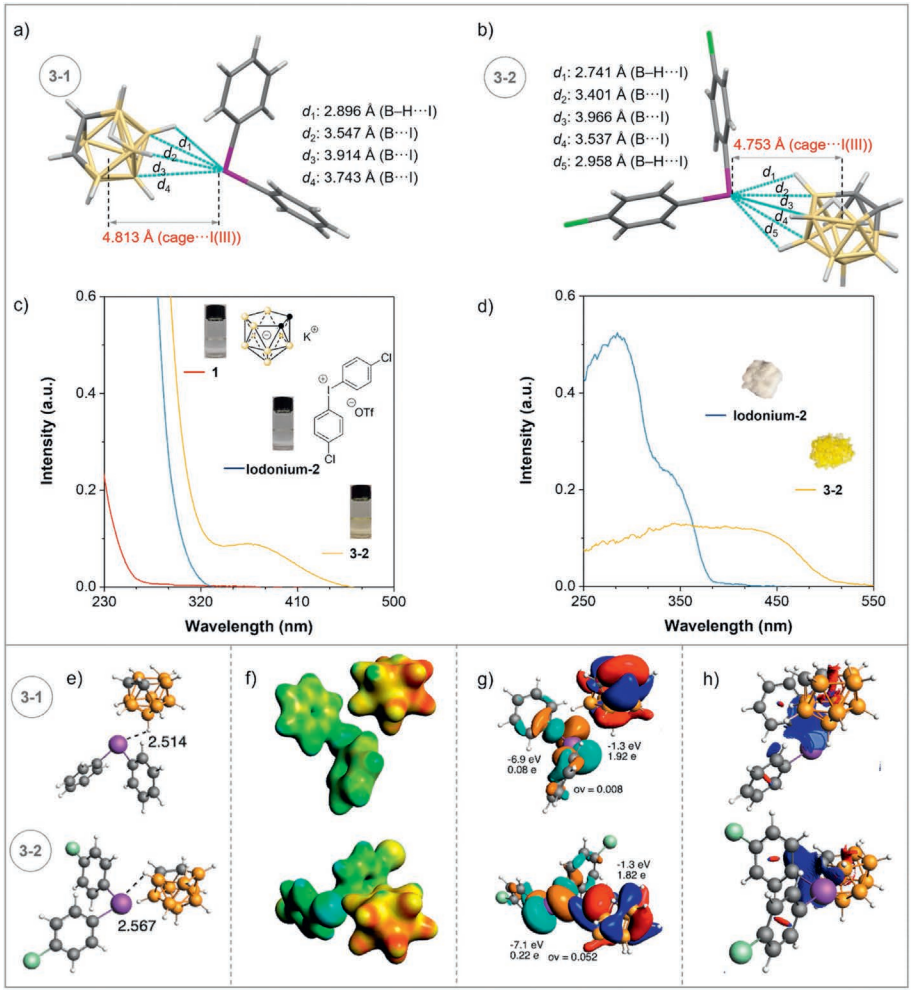


Fig. 2. (a, b) The crystal structures of **3–1** and **3–2**. (c) UV–vis spectra of **1**, **iodonium-2**, and **3–2** ($c = 5 \times 10^{-4}$ mol/L) in methanol. (d) UV–vis spectra of **iodonium-2** and **3–2** in the crystalline state. Insets are the photographs of **iodonium-2** and **3–2** in the methanol and crystalline state. (e) Geometries of systems **3–1** and **3–2** in **V** conformations. (f) Molecular electrostatic potential isosurface (electronic density isovalue = 0.03 a.u.). (g) HOMO of *nido* cage and LUMO of iodine molecule. Red and blue isosurfaces represent positive and negative phases for HOMO, whereas orange and turquoise for LUMO. Energies of the fragment molecular orbitals (in eV), gross Mulliken populations representing charge transfer in the complex (in e) and HOMO|LUMO overlaps (ov) are also enclosed. (h) NCI isosurface (isovalue = 0.5) of systems. Computed at ZORA-BLYP-D3(BJ)/TZ2P level of theory.

two conformations taken from the X-ray structure correspond to the vertex of the V-shaped iodine cation interacts with the cage, depicted in Fig. 2e. Energy decomposition analysis (EDA) reveals that the interaction between *nido*–carborane and hypervalent iodine is mainly electrostatic (Table S6 in Supporting information), with ΔV_{elstat} much larger than ΔE_{oi} in all cases (%elstat = 67–73 and %oi = 10–21). The nature of the interaction in terms of %elstat and %oi is very similar to that found in systems showing non-covalent cage···π interaction [91]. It has to be considered a non-covalent interaction despite the presence of a certain percentage of orbital (covalent) interactions. In vacuo, this positive charge is favored by directly interacting with the cage, thus avoiding certain repulsion between the boron cage and the negatively charged aromatic phenyl substituents of iodine fragment. This is further supported by the molecular electrostatic potential isosurfaces depicted in Fig. 2f. On the other hand, this bonding structure is also favored by the attractive orbital interactions. The most relevant interaction is between the highest occupied molecular orbital (HOMO) orbital of the *nido*–cage and the lowest unoccupied molecular orbital (LUMO) of the cationic iodine molecule (Fig. 2g). As a consequence of this interaction, we observed certain charge transfer from the *nido*–cage to the iodine unit in **3–1** and **3–2**. For completeness, the non-covalent interactions (NCI) isosurfaces [103] depicted in Fig. 2h allow us to better see the interactions for systems **3–1** and **3–2**.

The above results indicate the cage···I(III) interaction-induced charge transfer, which can modulate the electronic structure of carborane, thus might be useful for B–H bond functionalization. In light of this, we chose the hypervalent iodine reagent $PhI(OAc)_2$, which can dissociate in solution to generate the $(PhIOAc)^+$ species [104,105], to both promote the formation of the cage···I(III) interaction and control the strength of a cage···I(III) interaction. Theoretical calculations support the presence of a cage···I(III) interaction between the $(PhIOAc)^+$ group and *nido*–carborane group, as shown in the NCI isosurfaces (Fig. 3a). Notably, the charge transfer leads to a significant decrease of the charge in the carborane cage from −0.575 to −0.145, and from −0.087 to −0.003 for the H(B(9)) atom (Fig. 3a and Fig. S8a in Supporting information). The electronic effect can be utilized for further B–H bond functionalization and the formation of the B–I(III) bond, which is similar to the classic concerted metalation-deprotonation (CMD) in metal-mediated B–H functionalization [42–66]. Along this line, we investigated the reaction of *nido*–carborane and $PhI(OAc)_2$ in a solution of acetic acid and water. As a result, the B–I coupled product **3** was generated as confirmed by nuclear magnetic resonance (NMR) and high-resolution mass spectroscopy (HRMS) (Fig. 3b). This species

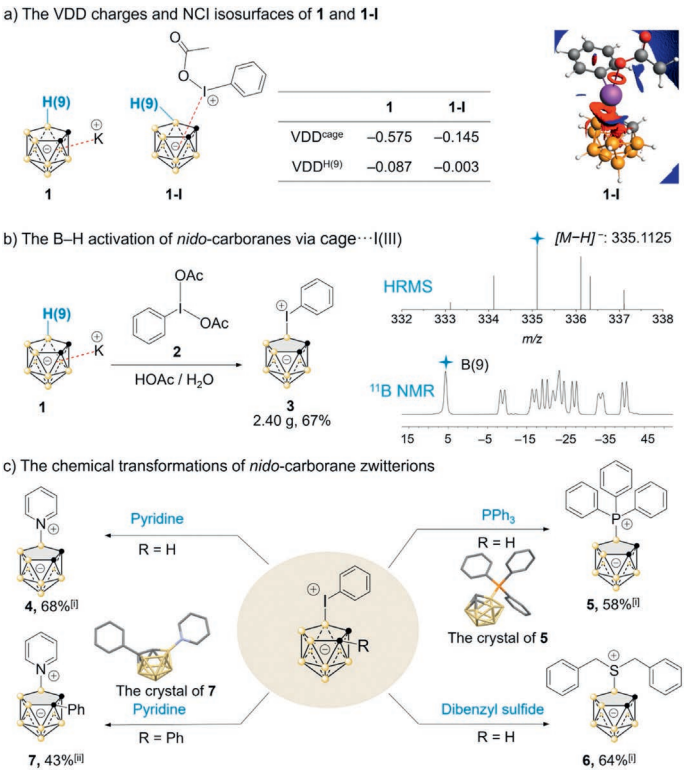


Fig. 3. (a) The selected VDD charges (in a.u.) and NCI isosurface (isovalue = 0.5) of **1** and **1-I**. Computed at ZORA-BLYP-D3(BJ)/TZ2P level of theory. (b) The B–H bond activation of *nido*–carborane *via* cage···I(III); the NMR and HRMS spectra of **3**. Reaction conditions: **1** (1.0 equiv., 10.0 mmol), $PhI(OAc)_2$ (1.0 equiv., 10.0 mmol), HOAc (20.0 mL), H_2O (12.0 mL), 0 °C, 30 min. (c) The chemical transformations of **3**. Reaction conditions: [i] **3** (1.0 equiv., 0.1 mmol), the nucleophiles (1.5 equiv., 0.15 mmol), methanol (1.0 mL), room temperature, 10 min. [ii] 7-Ph-7,8-$C_2B_9H_{11}^-$ (1.0 equiv., 0.1 mmol), $PhI(OAc)_2$ (2.0 equiv., 0.2 mmol), pyridine (1.5 equiv., 0.15 mmol), methanol (1.0 mL), room temperature, 10 min. The hydrogen atoms of crystal structures **5** and **7** are omitted for clarity.

is stable at a lower temperature and its preparation can be easily scaled up to a gram scale in a rapid manner (Fig. 3b). The subsequent substitution of B–I coupled products by nucleophiles, such as pyridine (**4**), triphenylphosphine (**5**), and dibenzyl sulfide (**6**), gave rise to the corresponding carborane derivatives in moderate to excellent yields under mild conditions (Fig. 3c). The compound **5** was further characterized by single-crystal X-ray diffraction, which unambiguously confirms the B(9) selectivity. Moreover, when a phenyl group is grafted on the carbon vertex of *nido*–carborane, the reaction preferentially occurs at the B(11)–H site. As exemplified by the crystal structure of **7**, the B(11)–H site is substituted, which is distant from the phenyl substituent. This should be attributed to the steric hindrance. The result differs from the oxidation coupling of *nido*–carborane in our previous report [74], which gave rise to a mixture of B(9)- and B(11)-functionalized products. For comparison, here the exclusive selectivity has been realized. Hence, the B–I coupled species could be used as a diverse reagent for further transformations.

Furthermore, theoretical calculations were conducted to elucidate the possible reaction pathway (Figs. S7 and S9 in Supporting information). The formation of the cage···I(III) interaction in the complex (**1-I**) is thermodynamically favorable, as indicated by an exergonic change of −6.0 kcal/mol. As the formation of the cage···I(III) interaction significantly reduces the negative charge of the carborane cage and the B(9)–H bond (Fig. S7), the B(9)–H bond functionalization is much more favored to form a B–I bond (compound **3**), accompanied by a further energy drop of 45.7 kcal/mol (Fig. S7). The further nucleophilic substitution by pyridine leads to a continued energy drop of 32.5 kcal/mol (Fig. S9). The calculations support the B–I containing compound as an intermediate or a reagent for subsequent synthetic applications. In addition, the intramolecular charge transfer effect from the carborane (HOMO) to the cationic substituent (LUMO) for compounds **3**–**7** has been demonstrated by theoretical calculations (Fig. S28 in Supporting information).

It is well known that benzoxazole is a crucial structural motif extensively utilized in the fields of biomedicine and photoelectric materials [106,107]. Given the distinctive electronic structure and enhanced physical properties exhibited by boron cage extension systems [64–66] compared to 2D aromatic ring-extended molecular structures, we attempted to construct the carborane-incorporated benzoxazole analogs with 2D-3D fused structures by the cage···I(III) interaction-mediated synthetic protocol. Despite the challenges associated with the direct B–O cross-coupling of boron cluster [42–83], the aforementioned synthetic objective might be reached by the cage···I(III) interaction-induced B–H bond functionalization and subsequent intramolecular cyclization. To our delight, the boron cage extended structure was achieved by using the amide-bearing *nido*–carborane **1a** as the sole starting material, $PhI(OAc)_2$ as the organoiodine(III) reagent and MeOH as the solvent at room temperature for 10 min, affording **2a** in 86 % isolated yield (Fig. 4). The molecular structure of **2a** was confirmed by SCXRD analysis to show an expected 3D carborane-fused benzoxazole. With the optimized conditions (Table S1 in Supporting information), we proceeded to explore the substrate scope. We were pleased to find that the *nido*–carborane substrates bearing *para*-substituted phenyl groups with various electron-donating substituents such as methyl (**2b**, **2n**, and **2o**), methoxy (**2c**), *n*-propyl (**2d**), tertbutyl (**2e**), trifluoromethoxy (**2f**) were well-tolerated, affording the desired products in excellent yields. In comparison, the electron-withdrawing substituents including halogen (**2h**–**2k**) and the ester group (**2l**) led to slightly decreased yields (67 %–83 %), which is attributed to the reduced nucleophilicity of the amide oxygen. Steric hindrance also affects the production, as indicated by a lower yield of **2m**. The substrates containing polycyclic and heteroaryl substituents, such as naphthyl (**2p**), pyridyl (**2q**), and thienyl (**2r**), are well tolerated. If the phenyl group is replaced by an alkyl substituent, the reaction also proceeds smoothly in a synthetically useful yield (**2s**). Additionally, the reaction is compatible with substrates bearing a chromophore like TPE (**2t**) or a pharmacophore derived from camphanic acid (**2u**). Moreover, a new 2D-3D fused structure with a six-membered heterocyclic ring (**2v**) was successfully synthesized by using the substrate bearing an embedded carbon atom. However, such cyclization does not occur when two electron-withdrawing substituents of fluorine appear in the *ortho*-substitution of phenyl (**2w**), indicating the electronic effect of the substituent on this reaction. Thus, a possible mechanism of the 5-*exo*-type annulation was proposed (Fig. S12 in Supporting information), which involves the cage···I(III) interaction-induced B–H bond activation, the formation of the crucial iodonium intermediate and intramolecular nucleophilic substitution. In contrast to our previous metal-catalyzed annulation to yield 2D-3D fusion [64–66], here the B–O closure is achieved by using a cheap organic compound of $PhI(OAc)_2$ instead of a noble metal catalyst.

The photophysical properties of the cyclized products were investigated for potential applications. To avoid the influence of the phenyl unit, **2s** was selected as a model for UV–vis spectral analysis (Fig. 5a). In contrast to compounds **1** and **1s**, the cyclized molecule of **2s** shows a new absorption peak around 270 nm, which arises from the charge transfer in the 2D-3D fused structure. The photoluminescence (PL) spectra of **2c**, **2g** and **2l** reveal that the substituent of the new molecular skeleton is able to evidently tune the energy level of the excited state. Specifically, the electron-

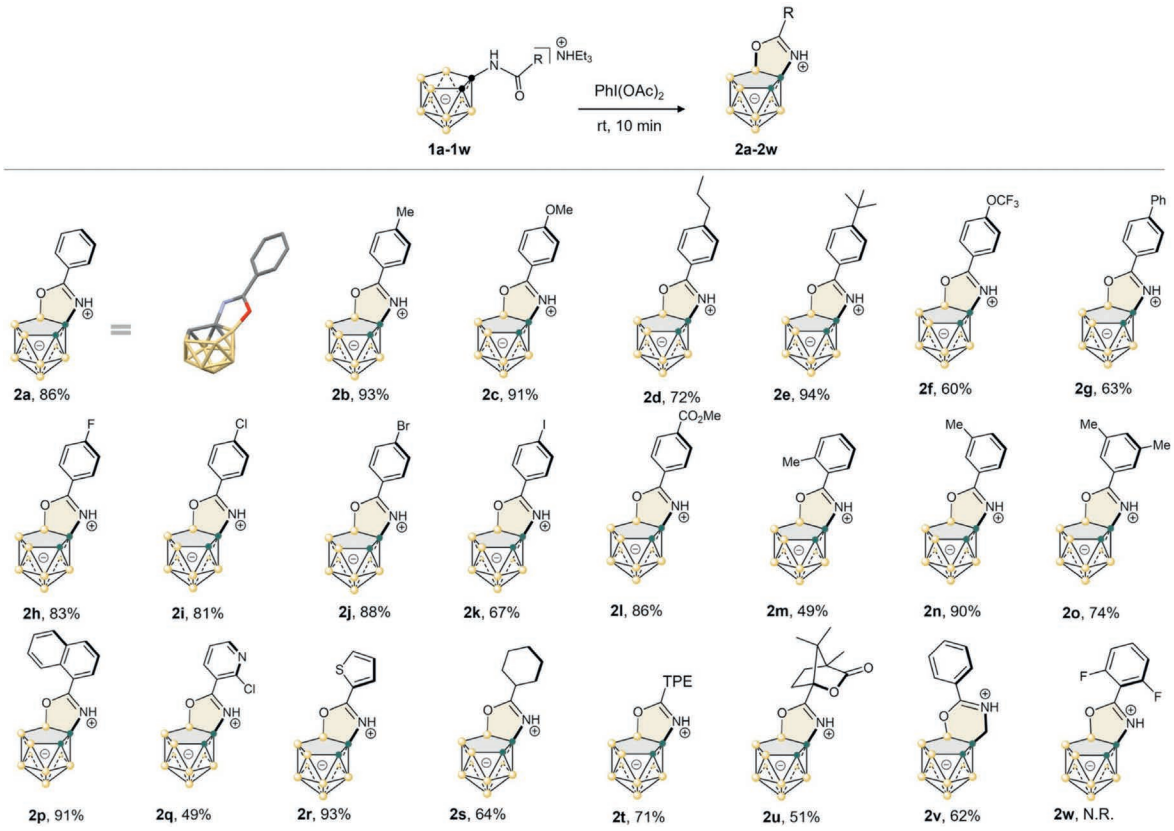


Fig. 4. Boron cage extension for the construction of 2D-3D fused molecular systems. Reaction conditions: **1a**-**1w** (1.0 equiv. 0.1 mmol), $PhI(OAc)_2$ (1.0 equiv., 0.1 mmol), MeOH (1.0 mL), room temperature, 10 min, affording **2a**-**2w** in 49 %–94 % isolated yields (see Supporting information for details). TPE = 4-(1,2,2-triphenylvinyl)phenyl.

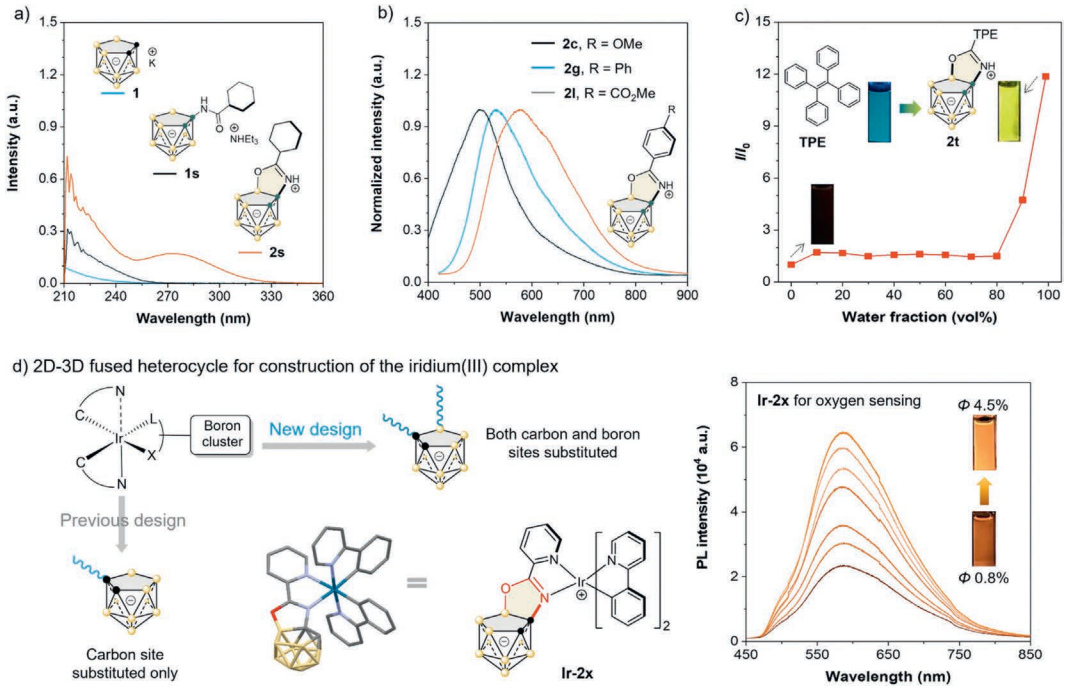


Fig. 5. (a) The UV–vis absorption spectra of **1**, **1s**, and **2s** in THF ($c = 100$ μmol/L). (b) The normalized PL spectra of compounds **2c**, **2g**, and **2l** ($\lambda_{ex} = 365$ nm). (c) Relative emission intensities of compound **2t** in THF/H_2O mixtures with increasing water volume fraction to 99 % ($c = 100$ μmol/L, $\lambda_{ex} = 365$ nm). (d) Molecular and crystal structures of the iridium(III) complex **Ir-2x** constructed by the new ligand **2x**. The PL spectra of **Ir-2x** in degassed THF solution. Each curve was measured after 20 s nitrogen bubbling into the solution. Insets are the corresponding photographs upon excitation by a UV lamp.

donating substituents on the phenyl ring leads to a blueshift of the emission (as exemplified by **2c**, $\lambda_{em} = 500$ nm) in comparison to **2g** ($\lambda_{em} = 531$ nm), whereas the electron-withdrawing substituent induces a redshift of emission (as exemplified by **2l**, $\lambda_{em} = 579$ nm) (Fig. 5b). In addition, the TPE-derived compound **2t** not only displays the AIE property [108,109] but also exhibits yellow emission in the aggregate state (Fig. 5c), distinct from the blue emission of TPE. Furthermore, to illustrate the versatility and practicality of our methodology, we synthesized a new type of iridium(III) complex (**Ir-2x**) by using the carborane-based 2D-3D fused compound **2x** as a new ligand. The complex also shows oxygen sensing (Fig. 5d). Therefore, the molecular design described here significantly broadens the range of carborane-based phosphorescent iridium(III) complexes [110,111].

We have developed a new boron cluster-based cage···I(III) interaction between *nido*–carborane anion and hypervalent iodine cation. This interaction significantly modifies the electronic structure of the boron cluster, thus facilitating selective B–H functionalization to generate a reactive and isolable B–I(III) coupled intermediate. Here, the cage···I(III) interaction in the intermediate is reminiscent of the B–M bond observed in transition metal-mediated B–H bond activation. Furthermore, the B–I(III) containing intermediate is the crucial synthon to be used for construction of B–X (X = N, P, O, S) bonds. More importantly, using this reaction protocol, a new type of carborane-fused hetero-polycyclic compounds featuring a B–O bond has been synthesized. These unprecedented 2D-3D fused structures demonstrate distinct photophysical properties with application potentials.

Declaration of competing interest

The authors declare that they have no known competing financial interests or personal relationships that could have appeared to influence the work reported in this paper.

CRediT authorship contribution statement

Ping Zhang: Writing – original draft, Methodology, Formal analysis, Data curation, Conceptualization. **Hongyuan Ren:** Writing – review & editing, Visualization. **Zhaofeng Sun:** Software. **Hou-Ji Cao:** Data curation. **Deshuang Tu:** Writing – review & editing, Funding acquisition. **Chang-Sheng Lu:** Writing – review & editing, Funding acquisition. **Jordi Poater:** Writing – review & editing, Funding acquisition. **Miquel Solà:** Writing – review & editing, Funding acquisition. **Hong Yan:** Writing – review & editing, Funding acquisition.

Acknowledgments

This work is supported by the National Natural Science Foundation of China (Nos. 92261202, 92461308, W2412072, 22201067 and 22401141), the Natural Science Foundation of Jiangsu Province (Nos. BZ2022007 and BK20241229), the Fundamental Research Funds for the Central Universities (No. 2024300362), Henan Normal University, TaiShan Industrial Experts Programme, the high-performance computing center of Nanjing University, the Spanish Ministerio de Ciencia, Innovación y Universidades (MCIN/AEI/10.13039/501100011033) (Nos. PID2022–138861NB-I00, PID2023-147424NB-I00, and CEX2021–001202-M), and the Generalitat de Catalunya (Nos. 2021SGR623 and 2021SGR224, and 2024 ICREA Academia prize for M.S.).

Supplementary materials

Supplementary material associated with this article can be found, in the online version, at doi:10.1016/j.cclet.2025.111617.

References

[1] Y. Zhu, A.T. Peng, K. Carpenter, et al., J. Am. Chem. Soc. 127 (2005) 9875–9880.
[2] R. Nuñez, M. Tarrés, A. Ferrer-Ugalde, et al., Chem. Rev. 116 (2016) 14307–14378.
[3] E.A. Qian, A.I. Wixtrom, J.C. Axtell, et al., Nat. Chem. 9 (2017) 333–340.
[4] Y. Zhu, N.S. Hosmane, Angew. Chem. Int. Ed. 57 (2018) 14888–14890.
[5] A.B. Buades, V.S. Arderiu, D. Olid-Britos, et al., J. Am. Chem. Soc. 140 (2018) 2957–2970.
[6] X. Wei, M.J. Zhu, Z. Cheng, et al., Angew. Chem. Int. Ed. 58 (2019) 3162–3166.
[7] J. Ochi, K. Tanaka, Y. Chujo, Angew. Chem. Int. Ed. 59 (2020) 9841–9855.
[8] Z. Wu, J. Nitsch, J. Schuster, et al., Angew. Chem. Int. Ed. 59 (2020) 17137–17144.
[9] K. Tanaka, M. Gon, S. Ito, et al., Coord. Chem. Rev. 472 (2022) 214779.
[10] Y. Sha, Z. Zhou, M. Zhu, et al., Angew. Chem. Int. Ed. 61 (2022) e202203169.
[11] L. Ji, S. Riese, A. Schmiedel, et al., Chem. Sci. 13 (2022) 5205–5219.
[12] J. Krebs, A. Häfner, S. Fuchs, et al., Chem. Sci. 13 (2022) 14165–14178.
[13] M. Zhu, Q. Zhou, H. Cheng, et al., Angew. Chem. Int. Ed. 62 (2023) e202213470.
[14] N. Ding, Y.C. Liao, G. Wang, et al., CCS Chem. 5 (2023) 2922–2932.
[15] R. Huang, T. Liu, H. Peng, et al., Chem. Soc. Rev. 53 (2024) 6960–6991.
[16] I. Guerrero, C. Viñas, I. Romero, et al., Green Chem. 23 (2021) 10123–10131.
[17] Y. Liu, W. Dong, Z.H. Li, et al., Chem 7 (2021) 1843–1851.
[18] X. Tan, X. Wang, Z.H. Li, et al., J. Am. Chem. Soc. 144 (2022) 23286–23291.
[19] Y. Xu, Y. Yang, Y. Liu, et al., Nat. Catal. 6 (2023) 16–22.
[20] N.S. Hosmane, J.A. Maguire, Y. Zhu, M. Takagaki, Boron and Gadolinium Neutron Capture Therapy For Cancer Treatment, Ch. 9, World Scientific Publishers, Singapore, 2011, pp. 165–170.
[21] M.F. Hawthorne, A. Maderna, Chem. Rev. 99 (1999) 3421–3434.
[22] V.I. Bregadze, I.B. Sivaev, S.A. Glazun, Anticancer. Agents Med. Chem. 6 (2006) 75–109.
[23] P. Stockmann, M. Gozzi, R. Kuhnert, et al., Chem. Soc. Rev. 48 (2019) 3497–3512.
[24] M. Couto, C. Alamón, S. Nievas, et al., Chem. Eur. J. 26 (2020) 14335–14340.
[25] A. Marfavi, P. Kavianpour, L.M. Rendina, Nat. Rev. Chem. 6 (2022) 486–504.
[26] J. Li, Q. Sun, C. Lu, et al., Nat. Commun. 13 (2022) 2143.
[27] A.G. Beck-Sickinger, D.P. Becker, O. Chepurna, et al., Cancer Biother. Radiopharm. 38 (2023) 160–172.
[28] Y. Shi, Z. Guo, Q. Fu, et al., Nat. Commun. 14 (2023) 1884.
[29] C. Alamón, B. Dávila, M.F. García, et al., Mol. Pharm. 20 (2023) 2702–2713.
[30] W. Ma, Y. Wang, Y. Xue, et al., Chem. Sci. 15 (2024) 4019–4030.
[31] J. Chen, M. Xu, Z. Li, et al., Angew. Chem. Int. Ed. 64 (2025) e202413249.
[32] E.L. Hoel, M.F. Hawthorne, J. Am. Chem. Soc. 97 (1975) 6388–6395.
[33] V.I. Bregadze, V. Ts. Kampel, N.N. Godovikov, J. Organomet. Chem. 112 (1976) 249.
[34] R. Zhang, L. Zhu, G. Liu, et al., J. Am. Chem. Soc. 134 (2012) 10341–10344.
[35] Z. Wang, H. Ye, Y. Li, et al., J. Am. Chem. Soc. 135 (2013) 11289–11298.
[36] Y.F. Han, G.X. Jin, Acc. Chem. Res. 47 (2014) 3571–3579.
[37] A.R. Popescu, F. Teixidor, C. Viñas, Coord. Chem. Rev. 269 (2014) 54–84.
[38] P.F. Cui, Y.J. Lin, Z.H. Li, et al., J. Am. Chem. Soc. 142 (2020) 8532–8538.
[39] S.T. Guo, P.F. Cui, X.R. Liu, et al., J. Am. Chem. Soc. 144 (2022) 22221–22228.
[40] J. Jiao, P. He, T. Yang, et al., Org. Chem. Front. 10 (2023) 5965–5970.
[41] R.N. Grimes, Carboranes, Elsevier Science, Amsterdam, 2016.
[42] N.S. Hosmane, R.D. Eagling, Handbook of boron science: with applications in organometallics, catalysis, materials and medicine, World Scientific, London, 2018, pp. 135–155.
[43] T.B. Marder, Ph.D. Thesis, University of California, 1981.
[44] J.D. Hewes, C.W. Kreimendahl, T.B. Marder, et al., J. Am. Chem. Soc. 106 (1984) 5757–5759.
[45] M.G.L. Mirabelli, L.G. Sneddon, J. Am. Chem. Soc. 110 (1988) 449–453.
[46] V.I. Bregadze, Chem. Rev. 92 (1992) 209–223.
[47] Z.Z. Qiu, Y.J. Quan, Z. Xie, J. Am. Chem. Soc. 135 (2013) 12192–12195.
[48] D. Olid, R. Núñez, C. Viñas, et al., Chem. Soc. Rev. 42 (2013) 3318–3336.
[49] Y. Quan, Z. Xie, J. Am. Chem. Soc. 136 (2014) 7599.
[50] X. Zhang, H. Zheng, J. Li, et al., J. Am. Chem. Soc. 139 (2017) 14511–14517.
[51] F. Lin, J.L. Yu, Y. Shen, et al., J. Am. Chem. Soc. 140 (2018) 13798–13807.
[52] Z. Qiu, Z. Xie, Acc. Chem. Res. 54 (2021) 4065–4079.
[53] R.F. Cheng, J. Zhang, H.F. Zhang, et al., Nat. Commun. 12 (2021) 7146.
[54] P.F. Cui, X.R. Liu, S.T. Guo, et al., J. Am. Chem. Soc. 143 (2021) 5099–5105.
[55] K. Cao, T.T. Xu, J. Wu, et al., Inorg. Chem. 60 (2021) 1080–1085.
[56] H.J. Cao, X. Wei, F. Sun, et al., Chem. Sci. 12 (2021) 15563–15571.
[57] Y.N. Ma, Y. Gao, Y. Ma, et al., J. Am. Chem. Soc. 144 (2022) 8371–8378.
[58] C. Sun, J.Y. Lu, J. Lu, Inorg. Chem. 61 (2022) 9623–9630.
[59] Z. Yang, C. Sun, X. Wei, et al., ChemCatChem 14 (2022) e202101571.
[60] P.F. Cui, X.R. Liu, G.X. Jin, J. Am. Chem. Soc. 145 (2023) 19440–19457.
[61] H.C. Noh, C.E. Kim, K. Lee, et al., Org. Lett. 25 (2023) 6643–6648.
[62] M. Sun, L. Feng, J.Y. Lu, Org. Lett. 26 (2024) 3697–3702.
[63] J. Wu, K. Cao, Org. Biomol. Chem. 23 (2025) 3701–3711.
[64] Z. Sun, J. Zong, H. Ren, et al., Nat. Commun. 15 (2024) 7934–7945.
[65] M. Zhu, P. Wang, Z. Wu, et al., Chem. Sci. 15 (2024) 10392–10401.
[66] Z. Wang, J. Yu, J. Zhang, et al., Chem. Sci. 16 (2025) 3705–3712.
[67] D.C. Young, D.V. Howe, M.F. Hawthorne, J. Am. Chem. Soc. 91 (1969) 859–862.
[68] O. Tutusaus, F. Teixidor, R. Núñez, et al., J. Organomet. Chem. 657 (2002) 247–255.
[69] M.Y. Stogniy, E.N. Abramova, I.A. Lobanova, et al., Collect. Czech. Chem. Commun. 72 (2007) 1676–1688.

[70] R. Frank, A.K. Adhikari, H. Auer, et al., Chem. Eur. J. 20 (2014) 1440–1446.
[71] P. Kaszynski, B. Ringstrand, Angew. Chem. Int. Ed. 54 (2015) 6576–6581.
[72] D. Zhao, Z. Xie, Angew. Chem. Int. Ed. 55 (2016) 3166–3170.
[73] M.Y. Stogniy, S.A. Erokhina, K.Y. Suponitsky, et al., New J. Chem. 42 (2018) 17958–17967.
[74] Z.M. Yang, W.J. Zhao, W. Liu, et al., Angew. Chem. Int. Ed. 58 (2019) 11886–11892.
[75] H.A. Mills, J.L. Martin, A.L. Rheingold, et al., J. Am. Chem. Soc. 142 (2020) 4586–4591.
[76] L. Yang, B.B. Jei, A. Scheremetjew, et al., Angew. Chem. Int. Ed. 60 (2021) 1482–1487.
[77] M. Chen, D.S. Zhao, J.K. Xu, et al., Angew. Chem. Int. Ed. 60 (2021) 7838–7844.
[78] W. Guo, C. Guo, Y.N. Ma, et al., Inorg. Chem. 61 (2022) 5326–5334.
[79] S. Li, Z. Xie, J. Am. Chem. Soc. 144 (2022) 7960–7965.
[80] Y.N. Ma, H. Ren, Y. Wu, et al., J. Am. Chem. Soc. 145 (2023) 7331–7342.
[81] H. Ren, P. Zhang, J. Xu, et al., J. Am. Chem. Soc. 145 (2023) 7638–7647.
[82] W. Lu, Y. Wu, Y.N. Ma, et al., Inorg. Chem. 62 (2023) 885–892.
[83] Y. Sun, J. Zhang, Y. Zhang, et al., Chem. Eur. J. 24 (2018) 10364–10371.
[84] B. Yao, Z.L. Wang, H. Zhang, et al., J. Org. Chem. 77 (2012) 3336–3340.
[85] H. Wang, W. Wang, W.J. Jin, Chem. Rev. 116 (2016) 5072–5104.
[86] S. Li, X.D. Wang, Q.Q. Wang, et al., Cryst. Growth Des. 16 (2016) 5460–5465.
[87] J. Cao, X. Yan, W. He, et al., J. Am. Chem. Soc. 139 (2017) 6605–6610.
[88] S.Y. Zhuang, Y. Cheng, Q. Zhang, et al., Angew. Chem. Int. Ed. 59 (2020) 23716–23723.
[89] D.X. Wang, M.X. Wang, Acc. Chem. Res. 53 (2020) 1364–1380.
[90] M. Solà, Nat. Chem. 14 (2022) 585–590.
[91] D. Tu, H. Yan, J. Poater, et al., Angew. Chem. Int. Ed. 59 (2020) 9018–9025.
[92] X. Zhang, H. Dai, H. Yan, et al., J. Am. Chem. Soc. 138 (2016) 4334–4337.
[93] S. Xu, H. Zhang, J. Xu, et al., J. Am. Chem. Soc. 146 (2024) 7791–7802.
[94] E.A. Merritt, B. Olofsson, Angew. Chem. Int. Ed. 48 (2009) 9052–9070.
[95] B. Zhou, M.K. Haj, E.N. Jacobsen, et al., J. Am. Chem. Soc. 140 (2018) 15206–15218.
[96] B. Ye, J. Zhao, K. Zhao, et al., J. Am. Chem. Soc. 140 (2018) 8350–8356.
[97] A. Yoshimura, V.V. Zhdankin, Chem. Rev. 124 (2024) 11108–11186.
[98] H.-J. Zhai, B. Kiran, J. Li, et al., Nat. Mater. 2 (2003) 827–833.
[99] S. Erhardt, G. Frenking, Z. Chen, et al., Angew. Chem. Int. Ed. 44 (2005) 1078–1082.
[100] H.J. Zhai, Q. Chen, H. Bai, et al., Acc. Chem. Res. 47 (2014) 2435–2445.
[101] H.J. Zhai, Y.F. Zhao, W.L. Li, et al., Nat. Chem. 6 (2014) 727–731.
[102] T. Jian, X. Chen, S.D. Li, et al., Chem. Soc. Rev. 48 (2019) 3550–3591.
[103] E.R. Johnson, S. Keinan, P. Mori-Sánchez, et al., J. Am. Chem. Soc. 132 (2010) 6498–6506.
[104] A. Varvoglis, Chem. Soc. Rev. 10 (1981) 377–407.
[105] R.M. Moriarty, O. Prakash, Org. React. 54 (1999) 273–418.
[106] C.Y. Zhang, K. Cao, T.T. Xu, et al., Chem. Commun. 55 (2019) 830–833.
[107] R. Varkhedkar, F. Yang, R. Dontha, et al., ACS Cent. Sci. 8 (2022) 322–331.
[108] F.Y. Zhu, L.J. Mei, R. Tian, et al., Chem. Soc. Rev. 53 (2024) 3350–3383.
[109] K. Wang, H. Si, X. Du, et al., Adv. Funct. Mater. 35 (2025) 2412856.
[110] J.C. Axtell, K.O. Kirlikovali, P.I. Djurovich, et al., J. Am. Chem. Soc. 138 (2016) 15758–15765.
[111] Y.X. Zhu, R.Z. Yuan, H.N. Zhang, et al., Chem. Eur. J. 30 (2024) e202401154.